Collision-free nonuniform dynamics within continuous optimal velocity models

Antoine Tordeux[*]
Jülich Supercomputing Centre, Forschungszentrum Jülich GmbH, Germany

Armin Seyfried[†]
Jülich Supercomputing Centre, Forschungszentrum Jülich GmbH, Germany
and Computer Simulation for Fire Safety and Pedestrian Traffic, Bergische Universität Wuppertal, Germany

(Received 13 June 2014; revised manuscript received 26 August 2014; published 21 October 2014)

Optimal velocity (OV) car-following models give with few parameters stable stop-and -go waves propagating like in empirical data. Unfortunately, classical OV models locally oscillate with vehicles colliding and moving backward. In order to solve this problem, the models have to be completed with additional parameters. This leads to an increase of the complexity. In this paper, a new OV model with no additional parameters is defined. For any value of the inputs, the model is intrinsically asymmetric and collision-free. This is achieved by using a first-order ordinary model with two predecessors in interaction, instead of the usual inertial delayed first-order or second-order models coupled with the predecessor. The model has stable uniform solutions as well as various stable stop-and -go patterns with bimodal distribution of the speed. As observable in real data, the modal speed values in congested states are not restricted to the free flow speed and zero. They depend on the form of the OV function. Properties of linear, concave, convex, or sigmoid speed functions are explored with no limitation due to collisions.

DOI: 10.1103/PhysRevE.90.042812 PACS number(s): 89.40.Bb, 05.45.−a, 45.70.Qj, 64.60.Cn

I. INTRODUCTION

Observations of congested road traffic flows present stable propagation of stop-and-go waves [1–3]. Such waves are observed on highways or during experiments (see, for instance, Ref. [4]), where the disturbance due to the infrastructure cannot explain their presence. They are also empirical features of pedestrian [5] as well as bicycle traffic [6]. This collective phenomenon is typical for the human driving. Stop-and-go waves are characterized by bimodal distributions of the velocity [7] and are observed within traffic [8,9] and pedestrian flows [5]. The modal speed values seem to depend on the density. Nowadays, the available empirical studies or theoretical investigations are not enough to explain the phenomena in sufficient detail.

Many approaches have been developed to understand road traffic flow (see, for instance, Refs. [10,11]). Traffic waves and instability were the topics of the pioneering papers in the 1950s and early 1960s [12]. The modeling of nonlinear traffic waves, instability, hysteresis, or more generally nonuniform solutions is one central point of the traffic research [13,14]. It is investigated with second-order, or higher-order, macroscopic models [15,16] as well as with kinetic mesoscopic ones [17,18]. Most of the studies are done with microscopic models. Traffic waves are the main field of cellular automaton models [19–21]. They are also described with delayed first-order or second-order continuous systems through stability analysis [3] or mapping to solitons [22].

One of the best investigated models is the optimal velocity (OV). The first OV models are car-following microscopic by delayed first-order [23] and second-order equations [24]. They are solely based on the optimal (or equilibrium) speed function and the reaction (or relaxation) time parameter. There exist microscopic discrete OV models [21,25] and macroscopic second-order [15,26] or hydrodynamical ones [27,28]. The OV models are simple, with few parameters that can be estimated from traffic data. Despite their simplicity, the obtained dynamics are rich and describe many empirical features [29,30].

The OV models have stationary uniform solutions that can be unstable. Yet, obtaining realistic nonuniform solutions with stop-and-go waves is not straightforward. Classical OV models can locally oscillate, leading to collisions or negative speed. These fortuitous colliding behaviors are different from the modeling of accidents (see Ref. [31]). They are unrealistic and have to be controlled. Unfortunately, collision-free stop-and-go patterns are limited to a small range of inputs with OV models. Only particular sigmoid optimal speed functions give collision-free solutions with traffic waves and multibunch phenomena [24,32,33]. This is due to the use of models with inertia (delayed first-order or second-order models), for which the vehicles do not monotonically stop for all initial conditions and values of the parameters. The occurrence of collisions prevents one from describing the space phase of the OV models well and restricts the use and calibration. These deficiencies are clearly established and have been debated in the literature [34–37].

Extensions of the OV models allow one to solve the problems (see, for instance, the microscopic models in Refs. [38,39] or the macroscopic models in Refs. [40,41]), but with the drawback of increasing the number of model parameters. At present, there is no consensus for one or another extended model. It is also unclear whether a higher modeling complexity is necessary to obtain realistic stop-and-go waves with a large range of parameters.

In this article, we develop a new generic and minimal OV model intrinsically asymmetric and collision-free for any value of the parameters. This is achieved by using

[*]a.tordeux@fz-juelich.de
[†]a.seyfried@fz-juelich.de

a continuous first-order ordinary equation system with no inertia and considering two predecessors for the interaction. The model has stationary uniform solutions with the same stability condition as classical models, as well as various stable nonuniform solutions (limit-cycle) with collision-free stop-and-go patterns. We propose to explore the space phase of the model analytically and by simulation. The article is organized as follows. In the Sec. II, we discuss classical OV models regarding the difficulties in combining collision-free property with the instability of a uniform solution. Then, the new OV model is defined. Section III concerns the stability analysis of the model. In Sec. IV, the nonuniform solutions, especially the distribution of the vehicle speed, are described by simulation according to the form of the parameters. A summary and conclusions are presented in Sec. V.

II. OPTIMAL VELOCITY MODELS

A. Classical models

The OV models are set by an optimal (or equilibrium) speed function V depending on the spacing (the difference of the central positions of a considered vehicle and the predecessor). The function describes how drivers regulate their speed. It is helpful to describe the dynamic of traffic systems but it is not derived from fundamental physical laws. On the one side, it contains strong physical constraints like the volume exclusion or finite desired speed, but it also contains factors determined by the perception and behavior of drivers. Classical modelings assume V such that

$$V(d) = 0, \ d \leqslant \ell, \quad \text{and} \quad V(d) \geqslant 0, \ d > \ell, \tag{1}$$

with finite limit value (the desired speed). $\ell > 0$ is the length of the vehicle. The most basic OV model [42] is of the first order:

$$\dot{x}_n(t) = V(\Delta x_n(t)), \tag{2}$$

where $x_n(t)$ is the position of the considered vehicle and $\Delta x_n(t) = x_{n+1}(t) - x_n(t)$ is the distance spacing of the vehicle n at time t ($n+1$ is the predecessor of the vehicle n, see Fig. 1).$\Delta x_n(t) - \ell$ is the distance gap of the vehicle n (the physical free distance with the predecessor). More realistic dynamics are obtained by introducing a delay time $\tau > 0$ in the model, corresponding to the observed driver and vehicle reaction time [23]:

$$\dot{x}_n(t+\tau) = V(\Delta x_n(t)). \tag{3}$$

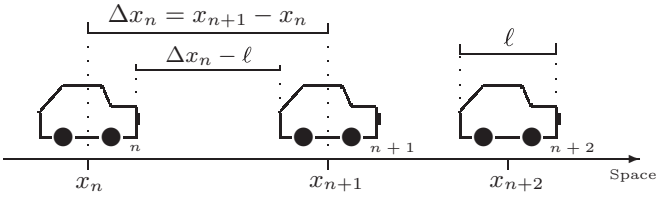

FIG. 1. Spacing variables: Vehicle length, ℓ; position, x; and distance spacing, Δx. The vehicle n collides with the vehicle $n+1$ if the distance gap $\Delta x_n(t) - \ell$ is negative.

Linear approximation of the delayed quantity in Eq. (3) leads to the second-order OV model [24], where the reaction time τ is considered as a relaxation time:

$$\ddot{x}_n(t) = \frac{1}{\tau}[V(\Delta x_n(t)) - \dot{x}_n(t)]. \tag{4}$$

The OV model (2) is solely based on the optimal speed function V while the models (3) and (4) also incorporate the reaction time parameter τ. More complex OV models exist with more parameters. See, for instance, the generalized force [38] or full velocity difference [39] models incorporating a speed difference term and two relaxation times, or even the multianticipative model [43] with $K \geqslant 1$ predecessors in interaction.

All OV models have uniform solutions $U(d)$ such that, for a given mean spacing $d > 0$,

$$\Delta x_n^U(t) = d, \quad x_n^U(t) = x_n^U(0) + tV(d), \tag{5}$$

for all n and all t. The uniform solution can be stable, when perturbations to uniform solutions vanish, or unstable. The analysis of the stability allows one to determine these properties according to the values of the parameters.

B. Stability and exclusion

The stability analysis of uniform solutions is variously used in the literature. The *local* stability analysis consists of describing the solution of a finite number of vehicles following a leader going at a constant speed. A line of vehicles (infinite in length or a ring) is considered for the *global* (or *collective*) stability analysis. The methods allows one to determine values of the parameters for a stable uniform solution. Both local and global stability conditions of the OV models are well know (see, for instance, Ref. [44]). Stability conditions are extracted by using linear approximations around uniform solutions. The method is related to the linear stability analysis.

Within the local stability analysis, we consider a vehicle, for which the leader moves at a constant speed v. One denotes $x(t)$ as the position of the vehicle at time $t \geqslant 0$ and $x_1(t) = x_1(0) + vt$ as the position of the leader. We assume $x(0) + \ell < x_1(0)$. Local analysis consists of determining conditions for which the solutions $x^U(t) = x_1(0) - d + tv$, with $V(d) = v$, are linearly stable. It can be used to formally control the presence of collision into the dynamics. This is done by considering the worst case where the leader is stopped ($v = 0$ and $d = \ell$). In this case the model is collision-free if it is stable, i.e., $x_1(t) - x(t) - \ell \to 0$, and if moreover the convergence is nonoscillating (i.e., $x_1(t) - x(t) - \ell > 0$ for all t). The basic first-order model (2) is locally linearly stable if $V'(d) > 0$. Moreover, it is nonoscillating and therefore collision-free. The conditions of the model with a reaction time are different. For the delayed model (3), the linear stability holds if $0 < \tau V'(d) < \pi/2$, while it is locally nonoscillating if

$$0 < \tau V'(d) < 1/e, \tag{6}$$

with $e = \exp(1)$ (see Ref. [45]). The second-order model (4) is locally linearly stable if $V'(d)$ and $\tau > 0$ and is locally nonoscillating if

$$0 < \tau V'(d) < 1/4, \tag{7}$$

(see, for instance, Ref [44]).

A line of vehicles (infinite or on a ring) is considered for the global stability analysis. It is well known that the basic model (2) is globally stable if $V'(d) > 0$. This assumption is natural for a model. The models (3) and (4) both have the following condition for global linear stability:

$$0 < \tau V'(d) < 1/2, \tag{8}$$

(see Refs. [24,45]). For sufficiently high reaction time τ, the models (3) and (4) can produce unstable uniform solutions. Yet, they are collision-free (i.e., locally nonoscillating) under more restrictive conditions (we have $\tau V' < 1/4 < 1/e < 1/2$). This means that the instability of uniform solutions for models with two parameters (τ and V') cannot be combined with a collision-free property. This can be argued by using the general second-order model with two parameters $\ddot{x}_n(t) = F[x_{n+1}(t) - x_n(t), \dot{x}_n(t)]$. If we denote $F : (d,v) \mapsto F(d,v)$ and the parameters $\alpha = \partial F/\partial d > 0$ and $\beta = \partial F/\partial v$, the condition $\beta^2 - 4\alpha > 0$, for which the model is locally nonoscillating, is incompatible with the condition for global instability of the uniform solution $\beta^2 - 2\alpha < 0$.

Many studies report the presence of collisions with classical OV models [24,33,35,36,46]. There exist extended OV models that can be simultaneously locally nonoscillating and globally unstable (see Refs. [38,39,44]). Yet, this is done by adding parameters to the dynamics that may be unnecessary for the modeling of realistic stop-and-go patterns.

C. Definition of a minimal collision-free OV model

The presence of collisions is hard to control with models of first order by delayed differential equation or models of second order. This is due to their inertia and tendency to locally oscillate. In contrast, it is easy to control the exclusion between the vehicles with ordinary first-order models. With these models, the collision-free property holds if the optimal speed function is positive and nil when the distance spacing is nil [see condition (1)]. However, they always have stable uniform solutions if they do not consider a reaction time. Therefore, our purpose is to develop an ordinary first-order OV model including a reaction time parameter.

The second-order OV model (4) can be obtained by applying a linear approximation around t to the left part of the delayed first-order model (3). Analytical and simulation results have shown that the dynamics obtained with OV models (3) and (4) are quite similar [32]. Here, we propose to apply a linear approximation to the right-hand side of Eq. (3) (by introducing the delay τ to the right). This leads to an implicit equation on the speed, sometimes related as the generalized optimal velocity (GOV) model

$$\dot{x}_n(t) = V[\Delta x_n(t) - \tau(\dot{x}_{n+1}(t) - \dot{x}_n(t))]. \tag{9}$$

The distance spacing is underestimated (respectively overestimated) in acceleration (deceleration) situations where the speed of the predecessor is higher (smaller) than the speed of the considered vehicle. These behaviors are what we expect of a reaction time parameter. The dynamics obtained with the GOV model should be close to those of the classical models (3) and (4). However, this speed model is not explicit. To approximate the solution of the implicit equation, the speeds in the right-hand side of the equation are substituted by the optimal speed function of the spacing:

$$\dot{x}_n(t) = V\{\Delta x_n(t) - \tau[V(\Delta x_{n+1}(t)) - V(\Delta x_n(t))]\}. \tag{10}$$

This model has two predecessors in interaction (the spacing Δx_{n+1} depends on the position of the second predecessor). It is solely based on the OV function and the reaction time parameter. The model is an explicit first-order version of the classical delayed or second-order OV models. The spacing of the predecessor is taken into account through the modeling of the reaction time. Oppositely to usual OV models including several predecessors in interaction, the goal here is not to increase the stability [43,47,48]. We aim to describe the unstable dynamics of the classical OV models by using a minimal collision-free model.

III. STABILITY ANALYSIS

In this section, we show on one hand that the minimal OV model (10) is collision-free simply if Eq. (1) is satisfied. On the other hand, we observe under the same assumption that the uniform solution can be unstable. This means that collision-free nonuniform solutions are possible with the model.

A. Local stability analysis and exclusion property

A leader vehicle travels at a constant speed v with a spacing d such that $V(d) = v$ for the local stability analysis. Its position at time t is $x_1(t) = x_1(0) + vt$. One denotes $x(t)$ as the position of the following vehicle. We assume $x(0) \leqslant x_1(0)$ and investigate the difference $x_1(t) - x(t) - d$. A linear expansion around the equilibrium point $[d, V(d)]$ gives $\dot{y}(t) = -\alpha y(t)$ with $\alpha = [1 + \tau V'(d)]V'(d)$. The solution converges to zero, i.e., the mean spacing d is stable, if $\alpha > 0$ [i.e., if $V'(d) > 0$]. The convergence is exponential with no oscillation. Therefore the OV model (10) comporting a reaction time $\tau > 0$ is locally collision-free if V is increasing.

The collision-free property of the model (10) can be shown without the requirement of linearization and weaker assumptions on V [49]. We introduce the continuous function $m(t) = \min_n \Delta x_n(t)$ with $m(0) \geqslant \ell$. If at any time $t \geqslant 0$, there exists unique n_0 such that $m(t) = \Delta x_{n_0}(t) = \ell$, then $m'(t) = V(\Delta \hat{x}_{n_0+1}(t)) - V(\Delta \hat{x}_{n_0}(t)) \geqslant 0$, with $\Delta \hat{x}_n(t) = \Delta x_n(t) + \tau[V(\Delta x_{n+1}(t)) - V(\Delta x_n(t))]$, if V satisfies assumption (1) (since in this case $V(\Delta \hat{x}_{n_0}(t)) = 0$ while $V(\Delta \hat{x}_{n_0+1}(t)) \geqslant 0$). This proves by continuity $m(t) \geqslant \ell$ for all t, and therefore the collision-free property

$$x_n(t) + \ell \leqslant x_{n+1}(t), \tag{11}$$

for all n and all t. Any solution of model (10), uniform or nonuniform, are by construction collision-free as soon as Eq. (1) holds, i.e., as soon as V is positive and nil when the spacing is smaller than the vehicle length ℓ. This is not the case for the classical OV models (3) and (4) for which collisions can appear even if Eq. (1) holds.

B. Global stability analysis

The global linear stability of uniform solutions (5) is analyzed for the collision-free OV model (10). N vehicles are considered on a ring of length L with mean spacing

$d = L/N > 0$. We denote $[x_1(t), \dots x_N(t)]$ the curvilinear positions of the vehicles at time t. $\Delta x_n(t) = x_{n+1}(t) - x_n(t)$ is the spacing of the vehicle n for all $1 \leqslant n < N$, and $\Delta x_N(t) = L + x_1(t) - x_N(t)$. The positions' differences $\tilde{x}_n(t) = x_n(t) - x_n^U(t)$ are analyzed for all $n = 1, \dots N$ to establish the stability of Eq. (5). A linear expansion around the equilibrium point $[d, V(d)]$ leads to the solution $[y_1(t), \dots y_N(t)]$ of the linear system

$$\dot{y}_n(t) = \alpha \Delta y_n(t) + \beta \Delta y_{n+1}(t), \tag{12}$$

where $1 \leqslant n \leqslant N$ and $y_{n+1}(t) = y_1(t)$ for $n = N$, $\alpha = [1 + \tau V'(d)]V'(d)$, and $\beta = -\tau[V'(d)]^2$. The uniform solution U is linearly stable if $y_n(t) \to 0$ when $t \to \infty$ for all n. The linear system is $\dot{\mathbf{y}}(t) = M\mathbf{y}(t)$ with M being an $N \times N$ circulant matrix. The eigenvalues of M are $\lambda_k = -[\alpha(1 - \iota_k) + \beta\iota_k(1 - \iota_k)]$, $\iota_k = \exp(i2\pi k/N)$ being the kth N root of the unit, $k = 0, \dots N - 1$. $\lambda_0 = 0$ and the system is linearly stable if $\mathrm{Re}(\lambda_k) < 0$ for all $k = 1, \dots N - 1$, denoting $\mathrm{Re}(\lambda_k) = V'(d)(1 - c_k)(ac_k - 1)$ as the real part of λ_k with $a = 2\tau V'(d)$ and $c_k = \cos(2\pi k/N)$. If $V'(d) > 0$, the sign of $\mathrm{Re}(\lambda_k)$ is the same as $ac_k - 1$. It is positive or nil if $V'(d) \leqslant 0$. Therefore $\mathrm{Re}(\lambda_k)$ is strictly negative for all $k = 1, \dots N - 1$ and all; i.e., the uniform solution is globally stable, if and only if

$$0 < \tau V'(d) < 1/2. \tag{13}$$

The condition is the same as that of the classical models (3) and (4). If the condition does not hold, there exists k such that $\mathrm{Re}(\lambda_k) > 0$ if

$$N > 2\pi / \cos^{-1}[1/(2\tau V'(\Delta))]. \tag{14}$$

A minimal number of vehicles is necessary to obtain nonuniform solutions. The solutions obtained with the collision-free OV model are described by simulation in the next section.

IV. NONUNIFORM SOLUTIONS

In this section the solutions of the new collision-free OV model (10) are calculated by simulation. The system on the ring in considered. We use the parallel explicit Euler scheme

$$x_n(t + \delta t) = x_n(t) + \delta t\, V\{\Delta x_n(t) - \tau[V(\Delta x_{n+1}(t)) - V(\Delta x_n(t))]\}, \tag{15}$$

with $1 \leqslant n \leqslant N$ and $\Delta x_{n+1}(t) = \Delta x_1(t)$, for $n = N$, and $\delta t = 10^{-3}\,s$ being the time step. The linear convergence of the discrete time system to the uniform solutions is shown in the Appendix. Here we describe the nonuniform solutions in the unstable situation where $\tau V'(d) > 1/2$ and Eq. (14) holds. A bounded linear optimal speed function is investigated before testing nonlinear functions.

A. Bounded linear optimal speed function

We first investigate the new OV model by using the basic bounded linear optimal speed function

$$V_l(d) = \min\{v_0, \max\{0, (d - \ell)/T\}\}, \tag{16}$$

with $\ell = 5\,\mathrm{m}$, $v_0 = 20\,\mathrm{m/s}$, $T = 1.5\,\mathrm{s}$, and $\tau = 1\,\mathrm{s}$. The values do not satisfy the stability condition (13).

A single experiment is done first. Twenty-two vehicles are observed on a 250-m-long ring from the uniform initial configuration with normal noise proportional to 0.5 m. A real experiment has been realized with similar conditions [4]. The real data show quick emergence and propagation of stop-and-go waves. Such an experiment was also performed with an extended OV car-following model [50] or the macroscopic Payne-Whitham model [51]. The trajectories obtained with the collision-free OV model are shown in Fig. 2. Stop-and-go waves also emerge. Two waves seem to develop into the simulation while only one is observed in the empirical data. Yet different initial conditions (for instance, a jam) allow one to obtain the propagation of only one wave into the system. The time at which stop-and-go occurs depends on the noise of the initial conditions. It can be long if initially the noise is very small. This single experiment of a transient state allows one to validate qualitatively the model with a bounded linear optimal speed. Further experiments have to be done to formally describe the model in a stationary state.

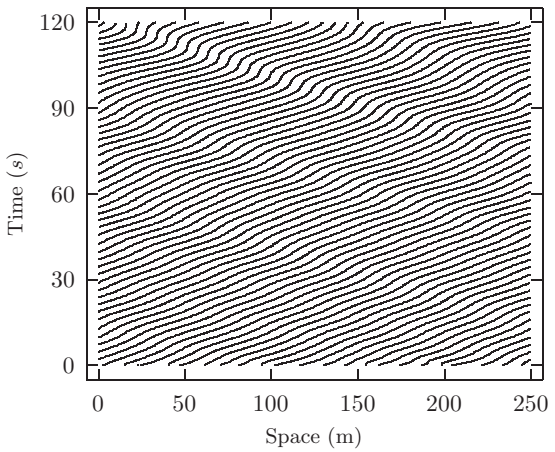

FIG. 2. Trajectories of 22 vehicles on a ring with the collision-free model and bounded linear OV function.

The distribution of the speeds is estimated in the stationary state (when $t \geqslant t_S = 10^6$ s) for various density levels. Here, deterministic results are obtained by taking jam initial conditions [where $x_{n+1}(0) - x_n(0) = \ell$ for all n excepted one]. First, the influence of the system size is investigated to exclude finite size effects. The vehicles' mean and modal speeds are plotted for $L = 505$, 1005, and 2005 m in Fig. 3. The modal speed values are calculated using Gaussian kernels and samples of size 5×10^5. As expected for this linear case, the mean speed is equal to the optimal speed $V_l(d)$. The two modal speeds are in general equal to the extremes $(0, v_0)$. They can only depend on the density level at the borders where $d \approx \ell$ and $d \approx d_0$ if the system is small. This phenomenon is attributed to the limited system size. For sufficiently large systems, the modal values of nonuniform solutions are constant, equal to $(0, v_0)$, for all congested density levels when the OV function is bounded linearly (see bottom panel of Fig. 3).

B. Non-linear optimal speed functions

The optimal speed functions tested in this section are nonlinear. They are all positive and increasing, nil when $d \leqslant \ell$ and equal to the desired speed v_0 when $d \geqslant d_0 = \ell + Tv_0$, with $\ell = 5\,\mathrm{m}$, $v_0 = 20\,\mathrm{m/s}$, $T = 1.5\,\mathrm{s}$. First, we use the convex

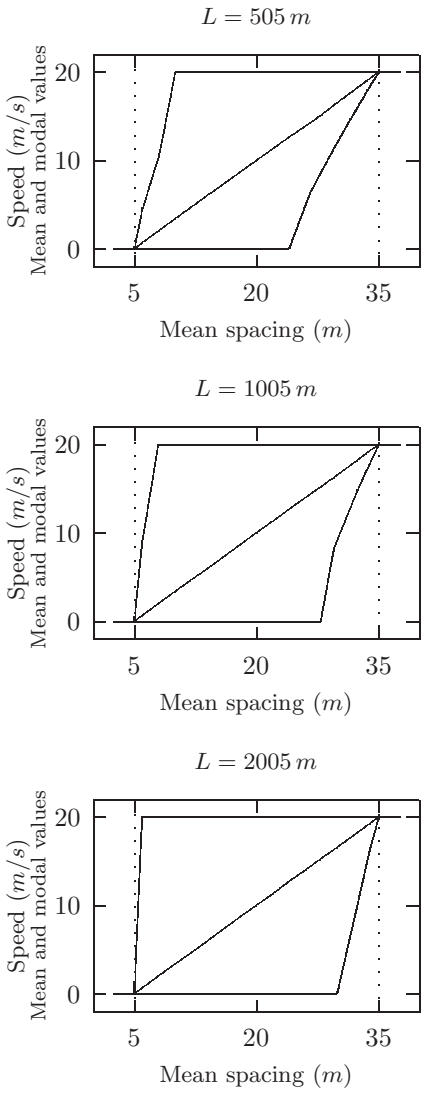

FIG. 3. Vehicle speeds according to the mean spacing in the stationary state for the bounded linear speed function (16) according to the size of the ring ($L = 505$, 1005, and 2005 m). The middle curve is the mean value, while upper and lower curves give the modal values. The vertical dotted lines correspond to the linear stability conditions.

function

$$V_v(d) = \begin{cases} 0, & d \leqslant \ell, \\ \frac{(d-\ell)^2}{v_0 T^2}, & \ell \leqslant d \leqslant d_0, \\ v_0, & d \geqslant d_0. \end{cases} \tag{17}$$

The derivative of the convex optimal speed function is linear $V_v'(d) = 2(d-\ell)/(v_0T^2)$ for $d \in [\ell, d_0]$ and nil elsewhere. If $\tau = 1$ s, the linear stability condition of the model (10) is $d < 16.25$ m. Next, we investigate the concave optimal speed function

$$V_c(d) = \begin{cases} 0, & d \leqslant \ell, \\ \frac{d-\ell}{T}\left[2 - \frac{d-\ell}{v_0 T}\right], & \ell \leqslant d \leqslant d_0, \\ v_0, & d \geqslant d_0. \end{cases} \tag{18}$$

The derivative of the concave optimal speed function is affine $V_c'(d) = 2/T - 2(d-\ell)/(v_0T^2)$ for $d \in [\ell, d_0]$ and is

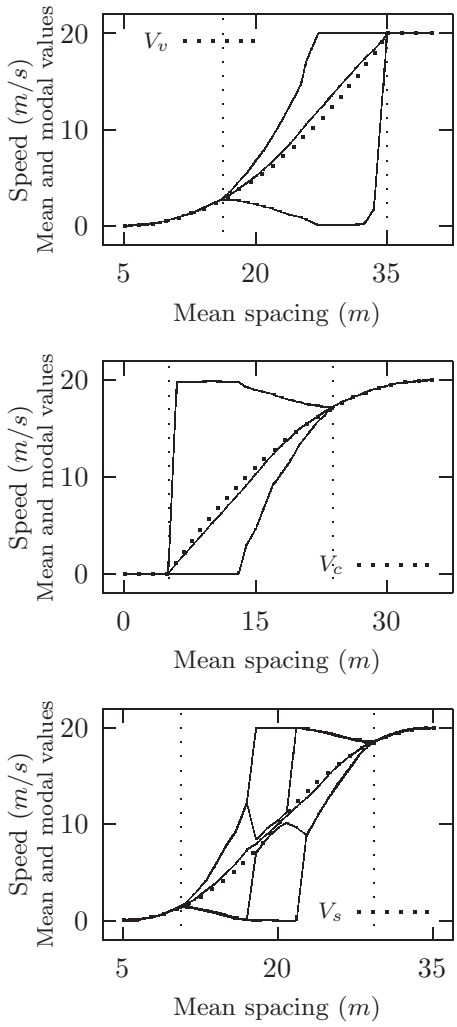

FIG. 4. Vehicle speeds according to the mean spacing in the stationary state for the nonlinear speed functions (17), (18), and (19). The middle curve is the mean value, while the upper and lower curves give the modal values. The vertical dotted lines correspond to the linear stability conditions. $L = 2005$ m.

nil elsewhere. The linear stability conditions leads to $d > 23.75$ m. Last, we use the sigmoid function

$$V_s(d) = \begin{cases} 0, & d \leqslant \ell, \\ 2\frac{(d-\ell)^2}{v_0 T^2}, & \ell \leqslant d \leqslant \ell + T v_0/2, \\ 2\frac{d-\ell}{T}\left[2 - \frac{d-\ell}{v_0 T}\right] - v_0, & \ell + T v_0/2 \leqslant d \leqslant d_0, \\ v_0, & d \geqslant d_0. \end{cases} \tag{19}$$

The derivative is bounded linear $V_s'(d) = 4(d-\ell)/(v_0T^2)$ for $d \in [\ell, \ell + Tv_0/2]$, $V_s'(d) = 4/T[1 - (d-\ell)/(v_0T)]$ for $d \in [\ell + Tv_0/2, d_0]$, and nil elsewhere. The stability does not hold if $10.625 < d < 29.375$ m.

The characteristics of the solutions obtained with nonlinear speed functions are described in Fig. 4. As previously, we mainly obtain bimodal distribution of the speed when the system is unstable. However, here the modal speed values depend on the mean spacing independently of the system size. This is not the case with the bounded linear V_l, where the modal

values are always equal to the extremes $(0, v_0)$ if the system is large enough. Modal speed values (or spacing) depending on the density are also observed with classical models through the form of the OV function [3,32], as well as with real data [8,9]. These results suggest that linear OV functions fail to describe the microscopic characteristic of realistic traffic waves.

When the optimal speed function is convex, the high mode of the speed's distribution can vary continuously with the spacing d from the mean to the maximal speed (see top panel of Fig. 4 and top panels of Fig. 5). A large range of values arise. The low mode remains close to zero. On the opposite, for concave speed function, the high mode is close to the maximal speed while the minimal one decreases continuously from the mean to zero by decreasing d (see center panel of Fig. 4 and center panels of Fig. 5). These two phenomena are observed by using sigmoid optimal speed. The high mode is regulated for low d where V_s is convex, while it is the lower one for high d where V_s is concave. In between, a continuous transition occurs from one shape of the distribution to the other. At the inflexion point, one observes simultaneously the two shapes with a double peak in the center and therefore a distribution with three modes (see bottom panel of Fig. 4 and bottom panels of Fig. 5). The diagram in Fig. 4 with sigmoid optimal speed V_s could be characterized by five different transitions indicating the occurrence of multimodal speed distributions and the reach of the extreme values. In the following we simplify this complexity to focus on the most interesting three phases of the model:

(1) free, where all the vehicles are at the desired speed;

(2) partially congested with slow-down-and-go waves (where "go" means that the vehicles move at a speed close to the desired one and "slow-down" means that the speed is between the desired speed and zero);

(3) fully congested with stop-and-slow-down waves (where "stop" means that the speed is close to zero).

A three-phase traffic theory has been developed by Kerner [52]. Here the third state, with go-and-slow-down waves, is not the *synchronous* one of the three-phase theory. However, different asymmetric sigmoid speed functions can give partially congested states of the model close to the free state with bimodal distributions of the speed and close modal values, or unimodal distributions. The repartition of the vehicles is relatively homogeneous and only one mode for the speed can be considered. This region could correspond to the synchronous state of three-phase theory. These aspects have to be explored in the light of real data and calibration of the OV function and also by using extensions of the model describing multilane traffic.

V. CONCLUSION

A new continuous OV car-following model is proposed for traffic applications. The model is a generic and minimal first-order one, based on the optimal speed function V and the reaction time parameter. In contrast to classical OV models, it does not produce local oscillating dynamics, and is intrinsically asymmetric and collision-free. This is achieved by using a first order system with two predecessors in the interaction, instead of usual inertial second order or delayed systems with one predecessor. The model shows that the modeling of collision-free traffic waves with a large range of parameters is possible with the minimalist OV framework, without adding superfluous parameters.

The model has the same stability condition of the uniform solution as classical OV models. It is unstable for a sufficiently high reaction time. Unstable solutions are nonuniform and collision-free, with the limit cycle describing realistic propagation of stop-and-go waves and bimodal distributions of the speed. The characteristics of the solutions, more precisely the modal speed values, are calibrated by the shape of the optimal speed function V. For bounded linear functions—and sufficiently large systems—the modal values of the speed are 0 and v_0 independently of the density. Using nonlinear V, the modal values continuously depend on the density level as observed in empirical data. This suggests that linear OV functions fail to describe realistic microscopic behaviors. The modal values can be regulated by using convex or concave functions. Sigmoid functions yield in an interesting two-phase congested traffic delimited by the inflexion point.

The modeling framework facilitates the description of stop-and-go waves and bimodal speed's distribution with the form of the optimal speed function. Statistical estimations and further model validations are necessary. Yet, the large range of collision-free nonuniform dynamics reproduced, the few and measurable parameters, and the low computational cost of the model make this approach useful for microscopic simulation of traffic or pedestrian flows, as well as for further theoretical investigations.

APPENDIX: GLOBAL STABILITY ANALYSIS IN DISCRETE TIME

The linear stability of uniform solutions is investigated in discrete time with the model (10). As previously, N vehicles are considered on a ring of length L. The discrete scheme (15), with $\delta t > 0$ the time step, is linearized leading to

$$y_n(t+\delta t) = y_n(t) + \delta t \times [\alpha \Delta y_n(t) + \beta \Delta y_{n+1}(t)], \quad \text{(A1)}$$

where $1 \leqslant n \leqslant N$ and $y_{n+1}(t) = y_1(t)$ for $n = N$, $\alpha = (1 + \tau V')V'$, and $\beta = -\tau(V')^2$, and by denoting $V' = V'(d)$ with $d = L/N$. This is $\dot{\mathbf{y}}(t+\delta t) = B\mathbf{y}(t)$, with $\mathbf{y}(t) = {}^{\mathrm{t}}[y_1(t), \ldots y_N(t)]$ and

$$B = \begin{bmatrix} 1-\delta t\alpha & \delta t(\alpha-\beta) & \delta t\beta & \\ & 1-\delta t\alpha & \delta t(\alpha-\beta) & \delta t\beta \\ \delta t\beta & & 1-\delta t\alpha & \delta t(\alpha-\beta) \\ \delta t(\alpha-\beta) & \delta t\beta & & 1-\delta t\alpha \end{bmatrix}.$$

The solution satisfies $\mathbf{y}(t) = B^{t/\delta t}\mathbf{y}(0)$. Here $B^{t/\delta t}$ can be easily calculated if B is diagonalizable. In this case, the solution converges towards the vector nil if the modules of the eigenvalues are strictly less than 1, except one equal to 1. Since the matrix B is circulant, the eigenvectors of the matrix are powers of N roots of the unit and the eigenvalues are

$$\lambda_k = 1 - \delta t[\alpha(1-\iota_k) + \beta\iota_k(1-\iota_k)], \quad \text{(A2)}$$

with $\iota_k = \exp(i2\pi k/N)$, $k = 0, \ldots N-1$. We have $\lambda_0 = 1$, $\mathrm{Re}(\lambda_k) = 1 - \delta t[\alpha(1-c_k) + \beta(c_k - c_{2k})]$, and $\mathrm{Im}(\lambda_k) = -s_k\delta t[\alpha - \beta(1-2c_k)]$, with $c_k = \cos(2\pi k/N)$ and $s_k = \sin(2\pi k/N)$. Here $|\lambda_k|^2 < 1$ if $\delta t < \delta(c_k) =: [\alpha + \beta(1+$

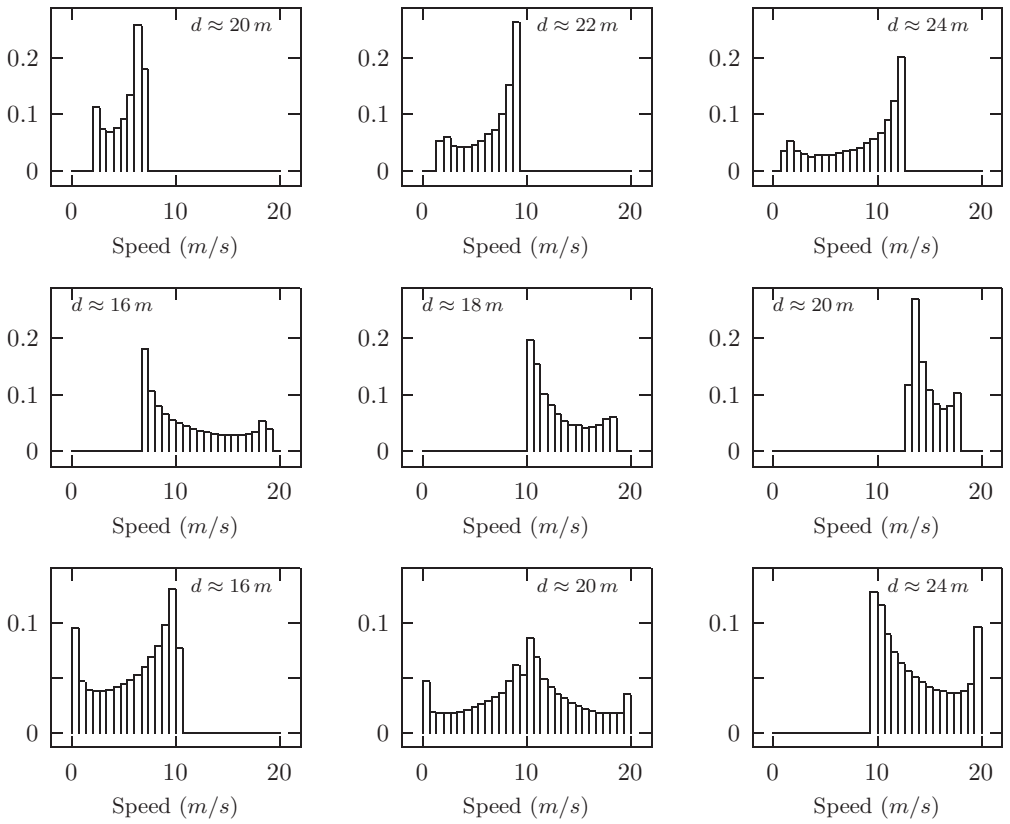

FIG. 5. Normalized histograms of the vehicles' speeds in the stationary state with varying d. From top to bottom: convex, concave, and sigmoid optimal speed functions.

$2c_k)](\alpha^2+\beta^2+2\alpha\beta c_k)^{-1}$. The maximal time step value must be less than $\min_k \delta(c_k)$ for the discretization to converge. This limit value must be strictly positive. The function δ is decreasing on $[-1,1]$ since $\delta'(x) = -2\beta^2(\alpha-\beta)(\alpha^2+\beta^2+2\alpha\beta x)^{-2} < 0$. $\delta(c_k)$ is minimal at the limit where $c_k \to 1$, i.e., for $k=1$ or $k=N-1$. One obtains

$$\delta t < \delta(c_1) \leqslant \frac{\alpha+3\beta}{(\alpha+\beta)^2} = \frac{1}{V'}(1-2\tau V'). \qquad \text{(A3)}$$

The inequality is an equality at the limit where $N \to \infty$. Assumption (A3) is a sufficient limit smallness condition of the time step for any finite system with $N < \infty$. It is the exact condition at the limit $N \to \infty$. Note that this bound is strictly positive if $V' > 0$ and $1 - 2\tau V' > 0$, which are the conditions for the linear stability of uniform solutions in the continuous time case. For $\tau = 0$, one obtains the well-known condition $\delta t < 1/V'$ of the discrete systems with no delay.

[1] J. Treiterer and J. Myers, in *Transportation and Traffic Theory: Proceedings of the Sixth International Symposium*, edited by D. J. Buckley (Elsevier Publishing Company, New York, 1974), pp. 13–38.

[2] B. S. Kerner and H. Rehborn, Phys. Rev. E **53**, R1297(R) (1996).

[3] G. Orosz, R. E. Wilson, and G. Stépán, Phil. Trans. R. Soc. London, Ser. A **368**, 4455 (2010).

[4] Y. Sugiyama, M. Fukui, M. Kikushi, K. Hasebe, A. Nakayama, K. Nishinari, and S. Tadaki, New J. Phys. **10**, 033001 (2008).

[5] A. Seyfried, A. Portz, and A. Schadschneider, in *Proceedings of the 9th International Conference on Cellular Automata for Research and Industry* (Springer-Verlag, Berlin, Heidelberg, 2010), pp. 496–505.

[6] J. Zhang, W. Mehner, E. Andresen, S. Holl, M. Boltes, A. Schadschneider, and A. Seyfried, Procedia Soc. Behav. Sci. **104**, 1130 (2013).

[7] J. Kaupuzs, R. Mahnke, and R. J. Harris, Phys. Rev. E **72**, 056125 (2005).

[8] W. F. Phillips, U.S.U.D. of Mechanical Engineering, and U.S.T.P. Bureau, *Kinetic Model for Traffic Flow*, Report (U.S. Department of Transportation Research & Special Programs Directorate, Transportation Programs Bureau, 1977).

[9] V. Aguiléra and A. Tordeux, J. Adv. Transp. **48**, 165 (2013).

[10] D. Chowdhury, L. Santen, and A. Schadschneider, Phys. Rep. **329**, 199 (2000).

[11] D. Helbing, Rev. Mod. Phys. **73**, 1067 (2001).

[12] D. C. Gazis, Oper. Res. **50**, 69 (2002).

[13] T. Li, Phys. D **207**, 41 (2005).

[14] R. E. Wilson and J. A. Ward, Transp. Plann. Technol. **34**, 3 (2011).

[15] H. J. Payne, in *Mathematical Models of Public Systems, Simulation Council Proceedings Series*, Vol. 1 (Simulation Councils, Incorporated, La Jolia, California, 1971), pp. 51–61.

[16] B. S. Kerner and P. Konhäuser, Phys. Rev. E **48**, R2335(R) (1993).
[17] R. Herman and I. Prigogine, Science **204**, 148 (1979).
[18] P. Nelson, Transp. Theory Stat. Phys. **24**, 383 (1995).
[19] K. Nagel and M. Schreckenberg, J. Phys. I **2**, 2221 (1992).
[20] A. Schadschneider and M. Schreckenberg, Ann. Phys. **509**, 541 (1997).
[21] D. Helbing and M. Schreckenberg, Phys. Rev. E **59**, R2505(R) (1999).
[22] T. Nagatani, Phys. Rev. E **61**, 3564 (2000).
[23] G. F. Newell, Oper. Res. **9**, 209 (1961).
[24] M. Bando, K. Hasebe, A. Nakayama, A. Shibata, and Y. Sugiyama, Phys. Rev. E **51**, 1035 (1995).
[25] M. Kanai, K. Nishinari, and T. Tokihiro, Phys. Rev. E **72**, 035102 (2005).
[26] D. Helbing, Eur. Phys. J. B **69**, 539 (2009).
[27] T. S. Komatsu and S.-I. Sasa, Phys. Rev. E **52**, 5574 (1995).
[28] M. Muramatsu and T. Nagatani, Phys. Rev. E **60**, 180 (1999).
[29] M. Schönhof and D. Helbing, Transport. Sci. **41**, 135 (2007).
[30] M. Treiber, A. Kesting, and D. Helbing, Transp. Res. B **44**, 983 (2010).
[31] S. H. Hamdar and H. S. Mahmassani, Transp. Res. Rec.: J. Transp. Res. Board **2088**, 45 (2008).
[32] K. Nakanishi, Phys. Rev. E **62**, 3349 (2000).
[33] I. Gasser, T. Seidel, G. Sirito, and B. Werner, Bull. Inst. Math. **2**, 587 (2007).
[34] C. F. Daganzo, Transp. Res. B **28**, 269 (1994).
[35] L. C. Davis, Phys. A **319**, 557 (2003).
[36] R. E. Wilson, P. Berg, S. Hooper, and G. Lunt, Eur. J. Phys. B **39**, 397 (2004).
[37] D. Helbing and A. F. Johansson, Eur. Phys. J. B **69**, 549 (2009).
[38] D. Helbing and B. Tilch, Phys. Rev. E **58**, 133 (1998).
[39] R. Jiang, Q. Wu, and Z. Zhu, Phys. Rev. E **64**, 017101 (2001).
[40] R. D. Kühne, in *Ninth International Symposium on Transportation and Traffic Theory*, edited by J. Volmuller and R. Hamerslag (CRC Press, Boca Raton, FL, 1984), pp. 21–42.
[41] D. Helbing, Phys. Rev. E **51**, 3164 (1995).
[42] L. A. Pipes, J. Appl. Phys. **24**, 274 (1953).
[43] H. Lenz, C. K. Wagner, and R. Sollacher, Eur. Phys. J. B **7**, 331 (1999).
[44] M. Treiber and A. Kesting, *Traffic Flow Dynamics* (Springer, Berlin, 2013).
[45] X. Zhang and D. F. Jarrett, Transp. Res. B **31**, 441 (1997).
[46] G. Orosz, R. E. Wilson, R. Szalai, and G. Stépán, Phys. Rev. E **80**, 046205 (2009).
[47] T. Nagatani, Phys. Rev. E **60**, 6395 (1999).
[48] Y. Hu, T. Ma, and J. Chen, Commun. Nonlinear Sci. Numer. Simul. **19**, 3128 (2014).
[49] R. Monneau, M. Roussignol, and A. Tordeux, Nonlinear Differ. Eqution Appl. **21**, 491 (2014).
[50] L. C. Davis, Phys. A (Amsterdam, Neth.) **390**, 943 (2011).
[51] M. R. Flynn, A. R. Kasimov, J.-C. Nave, R. R. Rosales, and B. Seibold, Phys. Rev. E **79**, 056113 (2009).
[52] B. S. Kerner, Phys. Rev. Lett. **81**, 3797 (1998).